

# J80-117 Unified Aerodynamic-Acoustic Theory for a Thin Rectangular Wing Encountering a Gust

Rudolph Martinez\* and Sheila E. Widnall†  
Massachusetts Institute of Technology, Cambridge, Mass.

A linear aerodynamic-acoustic theory is developed for the prediction of the surface pressure distribution and three-dimensional acoustic far-field for a flat plate rectangular wing encountering a stationary short-wavelength oblique gust. It is suggested that for an infinite-span wing, leading- and trailing-edge responses to a short-wavelength gust are essentially independent. This idea is used to solve for the two-dimensional pressure field due to the passage of an infinite-span wing through an oblique gust. By allowing the field point to come down to the wing's surface, one finds an expression for the surface pressure distribution which agrees with that given in the two-dimensional aerodynamic theories of Amiet and Adamczyk. Spanwise Fourier superposition of two-dimensional solutions to the infinite-span wing problem is used to approximate the three-dimensional acoustic field due to the interaction of a stationary oblique gust with a flat-plate rectangular wing traveling at a subsonic speed.

### Nomenclature

$b$	= wing semichord
$c_0$	= speed of sound
$D/Dt$	= substantial derivative
$E, E^*$	= complex combination of Fresnel integrals; $E^*$ denotes complex conjugate of $E$
$F$	= integrand factor, Eq. (39)
$\text{Im}$	= "imaginary part" of a complex number
$K$	= $\rho_0 w_0 U e^{-i\pi/4} / \sqrt{\pi} \sqrt{1-M^2} \sqrt{[k_x/(1-M^2)] + \mu}$ , a constant in Eqs. (21) and (22)
$k_x$	= reduced frequency or nondimensional chordwise wavenumber
$k_y, k_y^*$	= spanwise wavenumbers
$\ell$	= wing semispan
$M$	= Mach number
$P, p, p_*$	= perturbation pressures
$\bar{P}$	= Fourier transform of $p_*$ , Eq. (18b)
$\text{Re}$	= "real part" of a complex number
$t$	= time
$U$	= subsonic freestream velocity or velocity of the wing
$w, w_0$	= gust downwash on wing and its magnitude
$x, y, z, Z$	= chordwise, spanwise, and normal to wing spatial coordinates
$\Phi, \phi, \phi_*$	= perturbation velocity potentials
$\Lambda, \Lambda^*$	= interaction angles
$\mu$	= $\left\{ \frac{(k_x^2 + k_y^2) \sin^2 \Lambda}{(1-M^2)^2} \left[ \frac{M^2}{\sin^2 \Lambda} - 1 \right] \right\}^{1/2}$
$\rho_0$	= freestream density
$\omega$	= circular frequency
$\Psi$	= transformed velocity potential, Eq. (7b)
$\psi$	= $\tan^{-1}(\sqrt{x^2 + z^2}/y)$
$\theta$	= $\tan^{-1}(z/x)$
$\theta^*$	= $\tan^{-1}(\sqrt{1-M^2} z/x)$

### Superscripts

(1)	= solution to leading-edge problem
(2)	= solution to trailing-edge problem

### Subscripts

$a$	= acoustic reference frame
2-D	= two-dimensional solution
3-D	= three-dimensional solution

### Introduction

THE prediction of the unsteady loading induced on a thin planform of finite span interacting with a gust, and the associated acoustic field, is of fundamental interest due to its many applications. The versatility of the model lies in using the sinusoidal gust in question as a wavenumber component of a general, spatially frozen, upwash structure. Examples of such problems of current interest to aerodynamicists and acousticians include the calculation of forces on a wing (or a compressor blade) encountering turbulence, and the prediction of the acoustic field due to the helicopter blade-vortex interaction phenomenon.

In this paper we develop a linear aerodynamic-acoustic theory for the surface pressure distribution and three-dimensional acoustic far-field for the passage of a thin flat-plate rectangular wing through a stationary oblique gust of short wavelength.

The short-wavelength character of the gust considered introduces two important simplifications in the three-dimensional problem. First, it was pointed out in Ref. 1 that at high frequencies (small acoustic wavelength to chord ratio) the unsteady pressure distribution on a finite-span wing due to the interaction with the gust should differ little from that on a similar infinite-span wing except at small regions at the tips. Because of this, the two-dimensional problem for the pressure field due to the interaction of an oblique gust with an infinite-span wing is solved initially. Spanwise Fourier superposition of two-dimensional solutions of the infinite-span wing problem is then applied in such a way that the pressure distribution on the infinite wing's surface is given by the two-dimensional theory inside finite spanwise points and vanishes outside these spanwise points. The three-dimensional pressure field thus obtained is an approximation to that due to the passage of a rectangular wing through an oblique gust. The three-dimensional acoustic field, given in a coordinate system

Received April 13, 1979; revision received Sept. 17, 1979. Copyright © American Institute of Aeronautics and Astronautics, Inc., 1979. All rights reserved. Reprints of this article may be ordered from AIAA Special Publications, 1290 Avenue of the Americas, New York, N.Y. 10019. Order by Article No. at top of page. Member price \$2.00 each, nonmember, \$3.00 each. Remittance must accompany order.

Index categories: Nonsteady Aerodynamics; Noise; Aeroacoustics.

\*Research Assistant, Department of Aeronautics and Astronautics.

†Professor, Department of Aeronautics and Astronautics. Member AIAA.

fixed in the still fluid, is found by determining the asymptotic behavior of the pressure field as the field point goes to infinity.

The second simplification made possible by the high frequency character of the gust has to do with the solution technique applied to the two-dimensional problem for the pressure field due to the interaction of a gust with an infinite-span wing. At high frequencies, leading- and trailing-edge responses to the gust loading become essentially independent and their contribution to the total pressure field may be determined separately.

Landahl<sup>2</sup> has shown that the surface pressure distribution for an infinite-span wing passing through a gust of arbitrary wavelength may be determined by means of an iterative scheme applied in the aerodynamic reference frame (fixed on the wing). In the first step, the chord is allowed to extend infinitely in the downstream direction from the leading edge. This eliminates the Kutta condition and the wake from the problem. The solution to this "leading-edge problem," therefore, satisfies both the upstream boundary condition  $\Phi = 0$  and the flow tangency boundary condition: the vertical-velocity field on the wing's surface given by the solution cancels the gust downwash. Obviously, the leading-edge solution does not satisfy the condition of pressure continuity at the trailing edge and in the wake. Then, a "trailing-edge problem" must be posed in order to correct the leading-edge result: the chord is allowed to extend infinitely in the upstream direction from the trailing edge. The vertical-velocity field is now required to be zero on the wing's surface so that the superposition of leading- and trailing-edge solutions satisfies the condition of flow tangency. Also, the pressure given by the leading-edge solution is specified as a boundary condition on the semi-infinite line representing the trailing edge and the wake in the original problem. Adding the leading- and trailing-edge solutions, we obtain a result that satisfies the conditions of flow tangency on the wing's surface and pressure continuity at the trailing edge and in the wake. This solution, however, does not satisfy the upstream boundary condition  $\Phi = 0$ . Further iterations may be carried out to provide a more accurate solution.

Landahl<sup>3</sup> has shown that the series obtained by repeated application of the iteration scheme converges uniformly. As expected, due to the strong communication that exists between leading and trailing edges at low frequencies, many terms in the series are needed to give a good approximation to the solution for such a case. Investigators have resorted to other techniques to attack these problems.<sup>4-6</sup> For high frequencies, however, the leading and trailing edges behave almost independently of each other and few terms in the series are necessary to approximate the solution accurately. In the high-frequency limit, the solution is given by the first term in the series: the result from the leading-edge problem. It follows then that at very high frequencies the leading edge becomes the main source of acoustic radiation. In the past, the iteration scheme just described has been an essential tool in approaching high-frequency aerodynamic problems. The fundamental differences between the low and high frequency problems were explained in detail by Kaji.<sup>7</sup>

In 1972 Adamczyk<sup>8</sup> determined the acoustic far-field and surface pressure distribution for a thin airfoil interacting with a sound wave. The airfoil's span extended between two infinite parallel plates and thus both the surface pressure distribution and the acoustic field were essentially two-dimensional. The solutions were given in terms of infinite series of Mathieu functions evaluated at certain eigenvalues. Numerical results were presented for some values of the directivity in the aerodynamic reference frame showing enhancement of the acoustic signal in the downstream direction.

Adamczyk<sup>9</sup> has determined the response of an infinite-span swept wing to an oblique gust convected by a subsonic freestream. The expression for the pressure distribution on

the wing was given by the sum of the first two terms of the series from the iteration scheme. No acoustic analysis was performed.

Amiet<sup>1,10</sup> gave numerical results for the power spectral density of the three-dimensional acoustic far-field in the aerodynamic reference frame due to the interaction of small-scale turbulence with a rectangular flat-plate wing of finite span. His procedure was to replace the surface of the wing with a distribution of point dipoles of strength given by Adamczyk's<sup>9</sup> high-frequency airfoil-response function and to integrate over their acoustic far-fields. Amiet<sup>11</sup> estimated the power spectral density of the acoustic far-field due to a fast climbing rotor cutting through small-scale turbulence. The high-frequency character of the turbulence allowed him to consider spanwise blade elements as moving in a locally rectilinear fashion. The results were given in a coordinate system fixed to the rotor hub. Amiet<sup>12</sup> has also generalized Adamczyk's<sup>9</sup> original two-dimensional high-frequency aerodynamic theory by considering a gust not convected by the freestream. Plunging motion of the airfoil also was investigated in this work. No acoustic analysis was performed.

In the present theory, the first two terms in the series of the iteration scheme are used to estimate the pressure field everywhere due to the passage of an infinite-span wing through a short-wavelength oblique gust. Both the leading- and trailing-edge problems are solved in the aerodynamic reference frame by the Wiener-Hopf technique. The total solution obtained contains the aerodynamics of the wing surface, i.e., the surface pressure distribution, and the acoustics of the interaction in a rather compact analytic expression. Letting the field point in the solution come down to the wing's surface, we recover the two-dimensional aerodynamic results of Ref. 9 for the case of zero sweep. Letting the field point in the solution go to infinity, we obtain the two-dimensional acoustic field in the aerodynamic reference frame due to the interaction of a gust with an infinite-span wing. Spanwise Fourier superposition of two-dimensional solutions is used to approximate the three-dimensional pressure field for a rectangular wing passing through a stationary oblique gust of short wavelength. This last result is given in the acoustic reference frame, fixed in the still fluid. The three-dimensional acoustic far-field is obtained by allowing the observer's coordinates to go to infinity. The expressions are given in closed form and require no numerical computation.

It should be pointed out that expressions equivalent to those presented in this paper could be obtained by an alternate approach: To use the airfoil surface pressure distribution already available<sup>9,12</sup> as dipole strengths in a Green's function integral. By the present approach, however, the whole pressure field is obtained at once so that it is a more compact solution. Also, the results here in terms of contour integrals make the far-field calculations especially easy and unambiguous. For example, the phases of certain quantities are always obvious by the present complex variables method.

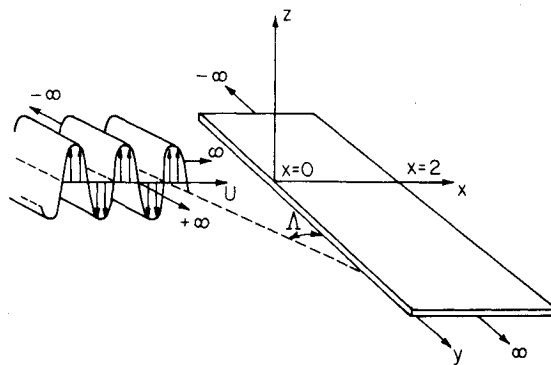


Fig. 1 The passage of an infinite-span wing through an oblique gust.

### Formulation

Following Amiet's formulation, in the aerodynamic reference frame we have a rigid flat-plate airfoil on the  $x$ - $y$  plane with its chord extending from  $x=0$  to  $x=2$ . It interacts at an angle  $\Lambda$  with a high-frequency sinusoidal gust convected by the freestream (Fig. 1). The linearized equation for the perturbation velocity potential  $\Phi$  is

$$\frac{\partial^2 \Phi}{\partial x^2} + \frac{\partial^2 \Phi}{\partial y^2} + \frac{\partial^2 \Phi}{\partial z^2} - \frac{1}{c_0^2} \frac{D^2 \Phi}{Dt^2} = 0 \quad (1)$$

with boundary conditions (B.C.s)

$$\Phi(x, y, 0, t) = 0 \quad \text{for } x < 0 \quad (2a)$$

$$\frac{\partial \Phi}{\partial z}(x, y, 0, t) = -bw(x, y)e^{i\omega t} \quad \text{for } 0 \leq x < 2$$

$$\text{and continuous} \quad \text{for all } x \quad (2b)$$

$$\frac{D\Phi}{Dt}(x, y, 0, t) = 0 \quad \text{for } x \geq 2 \quad (2c)$$

where the spatial variables have been non-dimensionalized with respect to the semichord  $b$ .  $D/Dt$  denotes  $\partial/\partial t + (U/b)\partial/\partial x$ , the linearized substantial derivative. For a sinusoidal gust of small amplitude  $w_0$ , the gust downwash  $w(x, y)$  becomes  $w_0 \exp\{i(\omega t - k_x x - k_y y)\}$ . For a gust convected by the freestream, the nondimensionalized gust wavenumber in the  $x$  direction  $k_x$  is then equal to  $\omega b/U$ , the reduced frequency; and the spanwise wavenumber  $k_y$  is  $(\omega b/U) \tan \Lambda$ . Boundary condition (2b) is thus a statement of flow tangency. From the linear relation between potential and pressure, i.e.,  $P = -\rho_0(D\Phi/Dt)$ , boundary condition (2c) requires that there be no pressure discontinuities at the trailing edge and in the wake.

Since the plate is infinite in the  $y$  direction, the potential  $\Phi$  will have the  $y$  dependence of the input gust, a traveling sinusoid; a harmonic behavior

$$\Phi(x, y, z, t) = \phi(x, z) \exp\{i(\omega t - k_y y)\}$$

is assumed according to Eq. (2b).

We also make the change of dependent variable

$$\phi(x, z) = \Phi_*(x, z) \exp\{ik_x M^2 x / (1 - M^2)\}$$

and compress the  $z$  coordinate by the change  $\sqrt{1 - M^2} z = Z$ . The object of these last two transformations is to reduce the relatively complicated convected wave equation to the familiar Helmholtz equation.

The boundary-value problem for  $\Phi_*$  becomes

$$\frac{\partial^2 \Phi_*}{\partial x^2} + \frac{\partial^2 \Phi_*}{\partial Z^2} + \mu^2 \Phi_* = 0 \quad (3)$$

B.C.s:

$$\Phi_*(x, 0) = 0 \quad \text{for } x < 0 \quad (4a)$$

$$\frac{\partial \Phi_*}{\partial Z}(x, 0) = \frac{-bw_0 \exp\{-ik_x x / (1 - M^2)\}}{\sqrt{1 - M^2}} \quad \text{for } 0 \leq x < 2$$

$$\text{and continuous} \quad \text{for all } x \quad (4b)$$

$$\left(\frac{ik_x}{1 - M^2} + \frac{\partial}{\partial x}\right) \Phi_*(x, 0) = 0 \quad \text{for } x \geq 2 \quad (4c)$$

where

$$\mu^2 = \frac{k_x^2 M^2}{(1 - M^2)^2} - \frac{k_y^2}{1 - M^2} = \frac{(k_x^2 + k_y^2)}{(1 - M^2)^2} \sin^2 \Lambda \left[ \frac{M^2}{\sin^2 \Lambda} - 1 \right]$$

and is one of the two wavenumber-related similarity parameters in the problem. The other is  $k_x / (1 - M^2)$ . The coefficient  $\mu^2$  is negative for  $M/\sin \Lambda < 1$ . This case corresponds physically to a subsonic speed of propagation of the disturbance due to the passage of the infinite-span wing through the stationary gust. Since a subsonically traveling disturbance radiates no sound, we expect no sound radiation for those Mach number and interaction angles for which  $\mu^2$  is negative.

### Leading-Edge Problem

The boundary-value problem for  $\Phi_*^{(1)}$ , the velocity-potential field due to the interaction of the gust with a semi-infinite chord airfoil extending downstream from the leading edge, is

$$\frac{\partial^2 \Phi_*^{(1)}}{\partial x^2} + \frac{\partial^2 \Phi_*^{(1)}}{\partial Z^2} + \mu^2 \Phi_*^{(1)} = 0 \quad (5)$$

B.C.s:

$$\Phi_*^{(1)}(x, 0) = 0 \quad \text{for } x < 0 \quad (6a)$$

$$\frac{\partial \Phi_*^{(1)}}{\partial Z}(x, 0) = -\frac{bw_0}{\sqrt{1 - M^2}} \exp\{-ik_x x / (1 - M^2)\} \quad \text{for } x > 0$$

$$\text{and continuous} \quad \text{for all } x \quad (6b)$$

The problem may be readily solved by the Wiener-Hopf technique. We define the transform pair

$$\Phi_*^{(1)}(x, Z) = \int_C \frac{d\lambda}{\sqrt{2\pi}} e^{-i\lambda x} \Psi(\lambda, Z) \quad (7a)$$

$$\Psi(\lambda, Z) = \int_{-\infty}^{\infty} \frac{d\xi}{\sqrt{2\pi}} e^{i\lambda \xi} \Phi_*^{(1)}(\xi, Z) \quad (7b)$$

where

$$\Psi(\lambda, Z) = \Psi_{\ominus}(\lambda, Z) + \Psi_{\oplus}(\lambda, Z)$$

that is,

$$\Psi_{\ominus}(\lambda, Z) = \int_{-\infty}^0 \frac{d\xi}{\sqrt{2\pi}} e^{i\lambda \xi} \Phi_*^{(1)}(\xi, Z) \quad (8a)$$

$$\Psi_{\oplus}(\lambda, Z) = \int_0^{\infty} \frac{d\xi}{\sqrt{2\pi}} e^{i\lambda \xi} \Phi_*^{(1)}(\xi, Z) \quad (8b)$$

The contour  $C$  and the regions of analyticity  $\ominus$ ,  $\oplus$  in the complex  $\lambda$  plane are yet to be determined by the physics of the problem. Transforming Eq. (5) and solving the resulting equation, we obtain that for this lifting problem

$$\Psi(\lambda, Z \pm) = \pm \Psi(\lambda, 0+) \exp\{\mp \sqrt{\lambda^2 - \mu^2} Z\} \quad (9)$$

where the branch of  $\sqrt{\lambda^2 - \mu^2}$  is chosen so that its argument vanishes as  $|\lambda|$  goes to infinity along  $C$ . We initially take  $\mu^2$  as a positive constant corresponding to  $M/\sin \Lambda > 1$ . The results obtained may be analytically continued later to include the negative  $\mu^2$  case.

Since an  $e^{i\omega t}$  time dependence was assumed, outward propagation requires that  $k_x$ , and thus also  $k_y$  and  $\mu$ , have a

small negative imaginary part. The regions of  $\oplus$  and  $\ominus$  analyticity in the complex  $\lambda$ -plane for Eqs. (8a,b) are then given by  $\text{Im}(\lambda) > \text{Im}(\mu)$ ,  $\text{Im}(\lambda) < \text{Im}(-\mu)$ , respectively, as shown in Fig. 2. The contour  $C$  runs below the real axis for  $\text{Re}(\lambda) < \text{Re}(-\mu)$  and above the real axis and the point  $\lambda = k_x / (1 - M^2)$  for  $\text{Re}(\lambda) > \text{Re}(\mu)$ .

From Eqs. (6a,b) and (8a,b) the following Wiener-Hopf equation is obtained ( $\ominus = \oplus$ )

$$\begin{aligned} & \frac{-ibw_0}{\sqrt{2\pi}\sqrt{1-M^2}\left(\lambda - \frac{k_x}{1-M^2}\right)} \left\{ \frac{1}{\sqrt{\lambda+\mu}} - \frac{1}{\sqrt{\frac{k_x}{1-M^2} + \mu}} \right\} \\ & + \frac{1}{\sqrt{\lambda+\mu}} \frac{\partial \Psi}{\partial Z} \ominus(\lambda, 0) \\ & = \frac{ibw_0}{\sqrt{2\pi}\sqrt{1-M^2}\left(\lambda - \frac{k_x}{1-M^2}\right)\sqrt{\frac{k_x}{1-M^2} + \mu}} \\ & - \sqrt{\lambda-\mu} \Psi \oplus(\lambda, 0+) \end{aligned} \quad (10)$$

the left side of Eq. (10) being a  $\ominus$  function and the right a  $\oplus$ . They are, therefore, analytic continuations of each other and so they are both at least entire. If  $\Psi$ ,  $\partial \Psi / \partial Z$  are assumed to be well behaved at  $\lambda = \infty$ , Liouville's theorem states that both sides of Eq. (10) are independently equal to zero. The right side then says that

$$\begin{aligned} \Psi(\lambda, 0+) &= \frac{ibw_0}{\sqrt{2\pi}} \frac{1}{\sqrt{1-M^2}} \frac{1}{\sqrt{\frac{k_x}{1-M^2} + \mu}} \\ &\times \frac{1}{\sqrt{\lambda-\mu}} \frac{1}{\left(\lambda - \frac{k_x}{1-M^2}\right)} \end{aligned} \quad (11)$$

and so, from Eqs. (9) and (7a)

$$\begin{aligned} \phi_*^{(1)}(x, Z) &= \frac{ibw_0}{2\pi\sqrt{1-M^2}} \frac{1}{\sqrt{\frac{k_x}{1-M^2} + \mu}} \frac{Z}{|Z|} \\ &\times \int_C \frac{d\lambda \exp\{-\sqrt{\lambda^2 - \mu^2}|Z| - i\lambda x\}}{\sqrt{\lambda-\mu}\left(\lambda - \frac{k_x}{1-M^2}\right)} \end{aligned} \quad (12)$$

Arguments similar to those made for the time- and  $y$ -dependence of the velocity potential are also applicable to the pressure. Together with the same changes of dependent and

independent variables used before for the potential, they give

$$P(x, y, z, t) = p(x, z) \exp\{i\omega t - ik_y y\} \quad (13a)$$

$$p(x, Z) = p_*(x, Z) \exp\{ik_x M^2 x / (1 - M^2)\} \quad (13b)$$

From the relationship between pressure and velocity potential, the pressure  $p_*^{(1)}(x, Z)$  corresponding to  $\phi_*^{(1)}(x, Z)$  is obtained

$$\begin{aligned} p_*^{(1)}(x, Z) &= \frac{-\rho_0 w_0 U}{2\pi\sqrt{1-M^2}} \frac{1}{\sqrt{\frac{k_x}{1-M^2} + \mu}} \frac{Z}{|Z|} \\ &\times \int_C \frac{d\lambda \exp\{-\sqrt{\lambda^2 - \mu^2}|Z| - i\lambda x\}}{\sqrt{\lambda-\mu}} \end{aligned} \quad (14)$$

For  $x > 0$ ,  $Z = 0+$ , the contour  $C$  may be deformed to  $C_1$  in Fig. 3 so that

$$\begin{aligned} p_*^{(1)}(x > 0, 0\pm) &= \frac{\mp \rho_0 w_0 U}{\sqrt{\pi}\sqrt{1-M^2}} \left( \frac{1}{\sqrt{\frac{k_x}{1-M^2} + \mu}} \right) \\ &\times \frac{\exp\{-\pi/4 - i\mu x\}}{\sqrt{x}} \end{aligned} \quad (15)$$

in agreement with the aerodynamic result in Ref. 9.

### Trailing-Edge Problem

The solution to the trailing-edge problem is a pressure  $p_*^{(2)}$ , such that  $p_*^{(1)} + p_*^{(2)}$  is zero at the trailing edge and in the wake.

From the linear relation between potential and pressure, we see that the pressure  $p_*^{(2)}(x, Z)$  also satisfies Helmholtz's equation. We require that  $\partial p_*^{(2)} / \partial Z$  vanish on the airfoil and that it be continuous for all  $x$ . With  $x = x' + 2$ , the trailing-edge correction boundary-value problem for  $p_*^{(2)}$  in the  $x' - Z$  coordinate system is

$$\frac{\partial^2 p_*^{(2)}}{\partial x'^2} + \frac{\partial^2 p_*^{(2)}}{\partial Z^2} + \mu^2 p_*^{(2)} = 0 \quad (16)$$

B.C.s:

$$\begin{aligned} \frac{\partial p_*^{(2)}}{\partial Z}(x' + 2, 0) &= 0 & \text{for } x' < 0 \\ &\text{and continuous} & \text{for all } x' \end{aligned} \quad (17a)$$

$$p_*^{(2)}(x' + 2, 0\pm) = -p_*^{(1)}(x' + 2, 0\pm) \quad \text{for } x' > 0 \quad (17b)$$

This problem is also solved by the Wiener-Hopf technique. We define the transform pair

$$p_*^{(2)}(x', Z) = \int_C \frac{d\lambda e^{-i\lambda x'}}{\sqrt{2\pi}} \tilde{P}(\lambda, Z) \quad (18a)$$

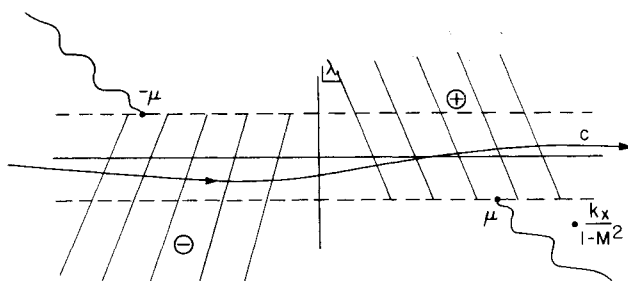


Fig. 2 Regions of analyticity  $\ominus$ ,  $\oplus$  and complex contour  $C$ .

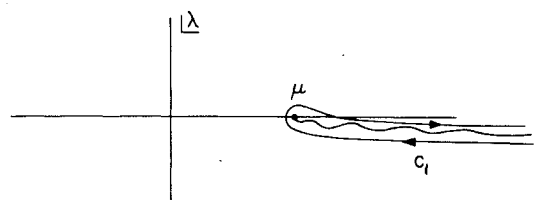


Fig. 3 Deformed contour  $C_1$ , for  $x > 0$ .

$$\tilde{P}(\lambda, Z) = \int_{-\infty}^{\infty} \frac{d\xi e^{i\lambda\xi}}{\sqrt{2\pi}} p_{*}^{(2)}(\xi, Z) \quad (18b)$$

where

$$\tilde{P}(\lambda, Z) = \tilde{P}_{\ominus}(\lambda, Z) + \tilde{P}_{\oplus}(\lambda, Z)$$

that is,

$$\tilde{P}_{\ominus}(\lambda, Z) = \int_{-\infty}^0 \frac{d\xi e^{i\lambda\xi}}{\sqrt{2\pi}} p_{*}^{(2)}(\xi, Z) \quad (19a)$$

$$\tilde{P}_{\oplus}(\lambda, Z) = \int_0^{\infty} \frac{d\xi e^{i\lambda\xi}}{\sqrt{2\pi}} p_{*}^{(2)}(\xi, Z) \quad (19b)$$

Transforming Eq. (16), solving the resulting equation and invoking the continuity of  $\partial p_{*}^{(2)}/\partial Z$  for all  $x'$ , we obtain

$$\tilde{P}(\lambda, Z \pm) = \pm \tilde{P}(\lambda, 0+) \exp\{\mp \sqrt{\lambda^2 - \mu^2} Z\} \quad (20)$$

where

$$\tilde{P}(\lambda, 0+) = \tilde{P}_{\ominus}(\lambda, 0+) + \tilde{P}_{\oplus}(\lambda, 0+)$$

the arbitrary function of  $\lambda$  to be determined by the Wiener-Hopf technique.

From boundary condition (17a), we see that  $\partial \tilde{P}_{\ominus}(\lambda, 0)/\partial Z = 0$ . From boundary condition (17b), and recalling the result in Eq. (15),  $\tilde{P}_{\oplus}(\lambda, 0 \pm)$  may be computed to be

$$\tilde{P}_{\oplus}(\lambda, 0 \pm) = \pm \frac{Ke^{-2i\lambda}}{\sqrt{\lambda - \mu}} \left\{ \frac{e^{i\pi/4}}{\sqrt{2}} - E[2(\lambda - \mu)] \right\} \quad (21)$$

where

$$E(a) \equiv \int_0^a \frac{dt}{\sqrt{2\pi t}} e^{it}$$

a Fresnel integral.  $E[2(\lambda - \mu)]$  thus has a branch point at  $\lambda = \mu$ .

The Wiener-Hopf equation for this problem is ( $\ominus = \oplus$ )

$$\sqrt{\lambda - \mu} \tilde{P}_{\ominus}(\lambda, 0+) + K \left[ \sqrt{\frac{\lambda + \mu}{\lambda - \mu}} e^{-2i\lambda} \left\{ \frac{e^{i\pi/4}}{\sqrt{2}} - E[2(\lambda - \mu)] \right\} - \frac{e^{-i\pi/4}}{\pi\sqrt{2}} \int_{\mu}^{\infty} \frac{d\xi}{\xi - \lambda} \sqrt{\frac{\xi + \mu}{\xi - \mu}} e^{-2i\xi} \right] = -\frac{1}{\sqrt{\lambda - \mu}} \frac{\partial \tilde{P}_{\oplus}}{\partial Z}(\lambda, 0+) - K f_{\oplus}(\lambda) \quad (22)$$

where  $K f_{\oplus}$  denotes that additive part of  $\sqrt{\lambda + \mu} \tilde{P}_{\oplus}(\lambda, 0+)$  which is analytic in the upper half  $\lambda$ -plane. Making the usual assumptions regarding the good behavior of  $\tilde{P}_{\ominus}(\lambda, 0+)$  and  $\partial \tilde{P}_{\oplus}(\lambda, 0)/\partial Z$ , we have that (Liouville's theorem) both sides of Eq. (22) are independently equal to zero. This gives  $\tilde{P}_{\ominus}(\lambda, 0+)$ . Adding Eq. (21) to it, we obtain  $\tilde{P}(\lambda, 0+)$  which upon substitution into Eq. (20) and by means of Eq. (18a) yields

$$p_{*}^{(2)}(x, Z) = \frac{-i\rho_0 w_0}{2\pi^2} \frac{U}{\sqrt{1-M^2}} \left( 1 / \sqrt{\frac{k_x}{1-M^2} + \mu} \right) \frac{Z}{|Z|} \int_C \frac{d\lambda}{\sqrt{\lambda + \mu}} \exp\{-\sqrt{\lambda^2 - \mu^2} |Z| - i\lambda(x-2)\} \int_{\mu}^{\infty} \frac{d\xi}{\xi - \lambda} \sqrt{\frac{\xi + \mu}{\xi - \mu}} e^{-2i\xi} \quad (23)$$

where the contour  $C$  is indented above the real axis at  $\lambda = \xi$ .

### Total Solution

Adding Eqs. (14) and (23) and applying Eq. (13b), we obtain the two-term approximation to the two-dimensional pressure field for the passage of an infinite-span wing through an oblique gust. Thus,

$$p(x, z) \cong p^{(1)}(x, z) + p^{(2)}(x, z) \quad (24)$$

The pressure distribution on the airfoil, that has its chord extending from  $x=0$  to  $x=2$ , is obtained from Eq. (24) which now says that

$$p(0 < x < 2, 0+) \cong p^{(1)}(x > 0, 0+) + p^{(2)}(x < 2, 0+) \quad (25)$$

The quantity  $p^{(1)}(x > 0, 0+)$  has already been determined and is given by Eqs. (15) and (13b). To obtain  $p^{(2)}(x < 2, 0+)$ , we start with Eq. (23) and observe that for  $Z=0+$ ,  $x < 2$ , the integral

$$I(\mu, x, Z+) = \int_C \frac{d\lambda}{\sqrt{\lambda + \mu}} \left[ \int_{\mu}^{\infty} \frac{d\xi}{\xi - \lambda} \sqrt{\frac{\xi + \mu}{\xi - \mu}} e^{-2i\xi} \right] \exp\{-\sqrt{\lambda^2 - \mu^2} Z - i\lambda(x-2)\} \quad (26)$$

may be deformed to

$$I(\mu, x, 0+) = \int_{C_2} \frac{d\lambda}{\sqrt{\lambda+\mu}} \exp[-i\lambda(x-2)] \int_{\mu}^{\infty} \frac{d\xi}{\xi-\lambda} \sqrt{\frac{\xi+\mu}{\xi-\mu}} e^{-2i\xi} \quad (27)$$

where  $C_2$  denotes the contour shown in Fig. 4.

Interchanging orders of integration we have

$$I(\mu, x, 0+) = - \int_{\mu}^{\infty} d\xi \sqrt{\frac{\xi+\mu}{\xi-\mu}} e^{-2i\xi} \int_{C_2} \frac{d\lambda}{\sqrt{\lambda+\mu}} \frac{e^{-i\lambda(x-2)}}{(\lambda-\xi)} \quad (28)$$

The term  $1/(\lambda-\xi)$  attains its highest value of  $-1/2\mu$  when  $\xi=\mu$  and  $\lambda=-\mu$ , and goes to zero as  $\xi \rightarrow \infty$  or as  $\lambda \rightarrow -\infty$  along  $C_2$ , or both. We can expect then that the largest contribution to  $I(\mu, x, 0+)$  comes from values of  $\xi$  near the lower limit. The following approximation is thus made

$$\begin{aligned} I(\mu, x, 0+) &\cong -\sqrt{2\mu} \exp[-i\mu(x-2)] \int_{\mu}^{\infty} \frac{d\xi - e^{-2i\xi}}{\sqrt{\xi-\mu}} \int_{C_2} \frac{d\lambda}{\sqrt{\lambda+\mu}} \frac{\exp[-i(\lambda-\mu)(x-2)]}{(\lambda-\mu)} \\ &= \sqrt{2\pi^{3/2}} \exp[-i\pi/4 - i\mu x] \{1 - (1+i)E^*[2\mu(2-x)]\} \end{aligned} \quad (29)$$

where  $E^*$  is the complex conjugate of  $E$  as defined in Eq. (21). Substituting for  $I(\mu, x, 0+)$  in  $p_*^{(2)}(x < 2, 0+)$ , we have

$$p_*^{(2)}(x < 2, 0+) \cong \frac{\rho_0 w_0 U \exp[-(i\pi/4) - i\mu x]}{\sqrt{2\pi} \sqrt{1-M^2}} \left( \frac{1}{\sqrt{\frac{k_x}{1-M^2} + \mu}} \right) \{1 - (1+i)E^*[2\mu(2-x)]\} \quad (30)$$

from which Eq. (25) becomes

$$p(0 < x < 2, 0\pm) \cong \mp \frac{\rho_0 w_0 U}{\sqrt{\pi} \sqrt{1-M^2}} \left( \frac{1}{\sqrt{\frac{k_x}{1-M^2} + \mu}} \right) \exp\left\{i\left[\frac{k_x M^2}{1-M^2} - \mu\right]x - \pi/4\right\} \left\{\frac{1}{\sqrt{x}} - \frac{1}{\sqrt{2}} [1 - (1+i)E^*[2\mu(2-x)]]\right\} \quad (31)$$

so that the Kutta condition is satisfied at  $x=2$  as required. The result in Eq. (31) agrees with that given in Ref. 9 for the pressure distribution on the infinite-span wing passing through an oblique short-wavelength gust. It serves as a check for the expression in Eq. (24), that we found for the pressure  $p(x, Z)$  at a general field point.

### Acoustic Far-Field Solutions

In this section, we start with the two-dimensional pressure field  $P(x, y, Z, t)$  due to the passage of an infinite-span wing through an oblique gust as given by Eqs. (24) and (13a). First, the two-dimensional far-field in the aerodynamic reference frame is determined by allowing the field point  $(x, Z)$  to go to infinity. The directivity of sound thus obtained is theoretically that which would be measured in a wind tunnel experiment. Second, we perform a spanwise Fourier superposition (over  $k_y$  wavenumbers) of two-dimensional pressure fields to approximate the three-dimensional pressure field for a wing of finite span passing through a short-wavelength gust at interaction angle  $\Lambda^*$ .

#### Two-Dimensional Acoustic Field in the Aerodynamic Reference Frame for an Infinite-Span Wing

From Eqs. (24) and (13a), we have

$$\begin{aligned} P(x, y, Z, t) &= -\frac{\rho_0 w_0 U}{2\pi \sqrt{1-M^2}} \frac{Z}{|Z|} \left( \frac{1}{\sqrt{\frac{k_x}{1-M^2} + \mu}} \right) \exp\left[i\left[\omega t - k_y y + \frac{k_x M^2 x}{1-M^2}\right]\right] \int_C d\lambda \left\{ \frac{1}{\sqrt{\lambda-\mu}} \right. \\ &\quad \left. + \frac{ie^{2i\lambda}}{\pi \sqrt{\lambda+\mu}} \left[ \int_{\mu}^{\infty} \frac{d\xi}{\xi-\lambda} \sqrt{\frac{\xi+\mu}{\xi-\mu}} e^{-2i\xi} \right] \right\} \exp\{-\sqrt{\lambda^2 - \mu^2} |Z| - i\lambda x\} \end{aligned} \quad (32)$$

We notice that, in order to obtain a non-vanishing far-field, the largest contribution to  $P(x, y, Z, t)$  as  $\sqrt{x^2 + Z^2} \rightarrow \infty$  must come from values of  $\lambda$  such that  $\lambda^2 - \mu^2 < 0$  or  $\lambda < \mu$ . It follows that in the far-field the largest contribution to the inside integral in Eq. (32) comes from its lower limit. Integrating by parts, we thus obtain that as  $\sqrt{x^2 + Z^2} \rightarrow \infty$

$$\int_{\mu}^{\infty} \frac{d\xi}{\xi-\lambda} \sqrt{\frac{\xi+\mu}{\xi-\mu}} e^{-2i\xi} \cong \frac{\pi \sqrt{2\mu} e^{-2i\lambda}}{\sqrt{\mu-\lambda}} \{1 - (1+i)E^*[2(\mu-\lambda)]\} \quad (33)$$

Substituting this into Eq. (32) the asymptotic behavior of the  $\lambda$  integral as  $\sqrt{x^2 + Z^2} \rightarrow \infty$  may be determined by steepest descents (Noble, <sup>13</sup> pp. 33-36) to be

$$\begin{aligned} \frac{P(x, y, z, t)}{\sqrt{x^2 + z^2} \rightarrow \infty} &\sim \sqrt{\frac{2}{\pi}} \frac{\rho_0 w_0 U \exp(i\omega t - ik_y y)}{\sqrt{1-M^2} \sqrt{\frac{k_x}{1-M^2} + \mu}} \frac{1}{(x^2 + z^2)^{1/4}} \exp\left[i\left[\frac{k_x M^2 \cos\theta}{1-M^2} - \mu \sqrt{1-M^2} \sin^2\theta\right] \sqrt{x^2 + z^2}\right] \\ &\quad \cdot \left\{ \frac{(1 - \cos\theta^*/2) e^{-i\pi/4} / \sqrt{2} - E^*[2\mu(1 - \cos\theta^*)]}{(1 - M^2 \sin^2\theta)^{1/4}} \right\} \end{aligned} \quad (34)$$

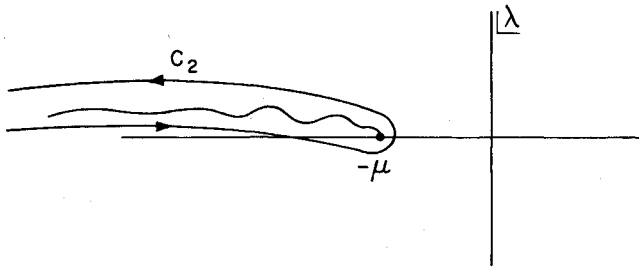


Fig. 4 Deformed contour  $C_2$ , for  $x < 2$ .

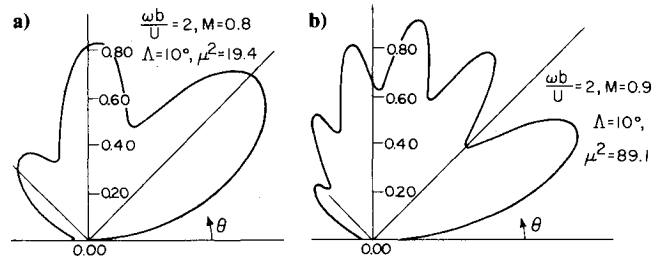


Fig. 5a, b Magnitude of the two-dimensional acoustic directivity,  $|D(\theta)|$ , in the aerodynamic reference frame for the passage of an infinite-span wing through an oblique gust.

where the substitution  $Z = \sqrt{1 - M^2} z$  has been made so that  $\theta = \tan^{-1}(z/x)$  and  $\theta^* = \tan^{-1}(\sqrt{1 - M^2} \tan \theta)$ . The expression in Eq. (34) shows that for negative  $\mu^2$  ( $\mu = -i\sqrt{-\mu^2}$ ) there is no acoustic field. We had anticipated that this should be the case since the disturbance due to the passage of the infinite-span wing through the gust then travels subsonically through the fluid. The quantity in brackets is the two-dimensional acoustic directivity  $D(\theta)$  in the aerodynamic reference frame. Plots of  $|D(\theta)|$  for different values of the Mach number  $M$  appear in Figs. 5a and b. For values of 0.3 m for the semi-chord  $b$  and 335 m/s for the speed of sound  $c_0$ , the cases in Figs. 5a and b correspond to frequencies of sound of about 280 Hz and 315 Hz, respectively.

### Three-Dimensional Acoustic Far-Field for a Rectangular Wing of Span $2\ell$

We start with the expression for the two-dimensional pressure field  $P(x, y, z, t)$ , given in Eq. (32), for the interaction of a gust with an infinite-span wing. We multiply the right side of Eq. (32) by the function

$$\sqrt{\frac{2}{\pi}} \frac{\sin(k_y - k_y^*)\ell/b}{k_y - k_y^*}$$

and integrate it with respect to  $k_y$  from  $-\infty$  to  $+\infty$ . Since the  $k_y$ -Fourier transform of

$$\sqrt{\frac{2}{\pi}} \frac{\sin(k_y - k_y^*)\ell/b}{k_y - k_y^*}$$

is  $\exp(-ik_y^*y)$  for  $|y| < \ell/b$  and zero everywhere else, it follows that if we apply the convolution theorem to our new  $P(x, y, Z=0, t)$ , we obtain a sinusoidal loading pattern of spanwise wavenumber  $k_y^*$  which ends abruptly at spanwise points  $y = \pm \ell/b$ . The velocity potential  $\Phi(x, y, Z, t)$  corresponds to this  $P(x, y, Z, t)$  is an approximation to the solution of Eq. (1) satisfying boundary conditions Eq. (2b), Eq. (2c) specified for  $|y| < \ell/b$ . In boundary condition Eq. (2b), the gust downwash  $w(x, y)$  now becomes  $w_0 \exp\{+i(\omega t - k_x x - k_y^* y)\}$ . The pressure distribution inside the spanwise points  $y = \pm \ell/b$  is given by the two-dimensional infinite-span wing aerodynamic results. This loading approximates well the pressure distribution on a three-dimensional finite-span wing passing through a short-wavelength gust at an interaction angle  $\Lambda^*$ . The pressure field obtained through the superposition, designated  $P_{3-D}(x, y, Z, t)$ , for points off the wing is then

$$P_{3-D}(x, y, Z, t) = \frac{1}{\pi} \int_{-\infty}^{\infty} dk_y \frac{\sin(k_y - k_y^*)\ell/b}{k_y - k_y^*} e^{-ik_y y} P_{2-D}(x, y, Z, t; k_y) \quad (35)$$

where  $P_{2-D}(x, y, Z, t; k_y)$  refers to that part of  $P(x, y, Z, t)$  in Eq. (32) not including the factor  $e^{-ik_y y}$ . Its indicated explicit dependence on  $k_y$  comes from interpreting  $\mu$  as

$$\mu(\omega, k_y) = \left\{ \left[ \frac{\omega b}{c_0(1 - M^2)} \right]^2 - \frac{k_y^2}{1 - M^2} \right\}^{1/2}$$

We now make the change of variable

$$\lambda = b\tilde{\lambda} + \frac{\omega b M}{c_0(1 - M^2)} \quad (36a)$$

$$d\lambda = b d\tilde{\lambda} \quad (36b)$$

so that

$$\sqrt{\lambda^2 - \mu^2} = \frac{ib}{\sqrt{1 - M^2}} \left\{ \frac{(\omega - \tilde{\lambda}U)^2}{c_0^2} - \tilde{\lambda} - \frac{k_y^2}{b^2} \right\}^{1/2} \quad (37)$$

Introducing Eqs. (36a, b) and (37) into Eq. (35), we obtain that the three-dimensional pressure field is

$$P_{3-D}(x, y, z, t) = -\frac{\rho_0 w_0}{2\pi^2} \frac{Ub}{\sqrt{1 - M^2}} \frac{z}{|z|} \exp(i\omega t) \int_{-\infty}^{\infty} \int_{C_a} d\tilde{\lambda} dk_y F(\omega, \tilde{\lambda}, k_y) \frac{\sin(k_y - k_y^*)\ell/b}{k_y - k_y^*} \times \exp \left[ -i\sqrt{\frac{(\omega - \tilde{\lambda}U)^2}{c_0^2} - \tilde{\lambda} - \frac{k_y^2}{b^2}} b|z| - i\tilde{\lambda}bx - ik_y y \right] \quad (38)$$

where  $C_a$  denotes the contour in the complex  $\tilde{\lambda}$ -plane obtained by shifting  $C$  according to Eqs. (36a, b). Introducing the far-field approximation given in Eq. (33), the factor  $F(\omega, \tilde{\lambda}, k_y)$  becomes

$$F(\omega, \tilde{\lambda}, k_y) = \frac{I}{\sqrt{\frac{\omega b}{U(1-M^2)} + \left\{ \left[ \frac{\omega b}{c_0(1-M^2)} \right]^2 - \frac{k_y^2}{1-M^2} \right\}^{1/2}}} \left\{ \frac{I}{\sqrt{b\tilde{\lambda} + \frac{\omega b M}{c_0(1-M^2)} - \left\{ \left[ \frac{\omega b}{c_0(1-M^2)} \right]^2 - \frac{k_y^2}{1-M^2} \right\}^{1/2}}} \right. \\ \left. + \frac{\frac{i\sqrt{2}\sqrt{1-M^2}}{b} \left\{ \left[ \frac{\omega b}{c_0(1-M^2)} \right]^2 - \frac{k_y^2}{1-M^2} \right\}^{1/4}}{\sqrt{\frac{(\omega - \tilde{\lambda}U)^2}{c_0^2} - \tilde{\lambda}^2 - \frac{k_y^2}{b^2}}} \left\{ 1 - (1+i)E^* \left[ 2 \left\{ \frac{\omega^2 b^2}{c_0^2(1-M^2)^2} - \frac{k_y^2}{1-M^2} \right\}^{1/2} - \frac{\omega b M}{c_0(1-M^2)} - b\tilde{\lambda} \right] \right\} \right\} \quad (39)$$

Next, we introduce a time-frequency Fourier transform into Eq. (38) that

$$P_{3-D}(x, y, z, t) = -\frac{\rho_0 w_0 U b}{2\pi^2 \sqrt{1-M^2}} \frac{z}{|z|} \int_{-\infty}^{\infty} \int_{C_a} d\tilde{\lambda} dk_y \int_{-\infty}^{\infty} d\omega' \delta[\omega' - (\omega - \tilde{\lambda}U)] F(\omega', \tilde{\lambda}, k_y) \\ \cdot \frac{\sin(k_y - k_y^*)\ell/b}{k_y - k_y^*} \exp \left[ -i\sqrt{\frac{\omega'^2}{c_0^2} - \tilde{\lambda}^2 - \frac{k_y^2}{b^2}} b|z| - i\tilde{\lambda}bx_a - ik_y y + i\omega' t \right] \quad (40)$$

where  $bx_a = bx - Ut$ , the  $a$  subscript denoting the acoustic reference frame.

Introducing one of the limiting forms of the delta function, e.g.,

$$\delta(\xi) = \lim_{\epsilon \rightarrow 0} \frac{\xi}{\epsilon^2 + \xi^2} \frac{1}{\pi}$$

into Eq. (40) and interchanging the limiting process with the integrals, which themselves may be interchanged, we obtain

$$P_{3-D}(x_a, y, z, t) = -\frac{\rho_0 w_0 U b}{2\pi^2 \sqrt{1-M^2}} \frac{z}{|z|} \lim_{\epsilon \rightarrow 0} \int_{-\infty}^{\infty} d\omega' e^{i\omega' t} \int_{-\infty}^{\infty} \int_{C_a} d\tilde{\lambda} dk_y \frac{\sin(k_y - k_y^*)\ell/b}{k_y - k_y^*} \\ \cdot \frac{1}{\pi} \frac{[\omega' - (\omega - \tilde{\lambda}U)]}{\{\epsilon^2 + [\omega' - (\omega - \tilde{\lambda}U)]^2\}} F(\omega', \tilde{\lambda}, k_y) \exp \left[ -i\sqrt{\frac{\omega'^2}{c_0^2} - \tilde{\lambda}^2 - \frac{k_y^2}{b^2}} b|z| - i\tilde{\lambda}bx_a - ik_y y \right] \quad (41)$$

The asymptotic behavior of  $P_{3-D}$  as  $\sqrt{x_a^2 + y^2 + z^2} \rightarrow \infty$  may be determined by the method of stationary phase (Ref. 14, p. 382). Applying the latter to the  $\tilde{\lambda}$  and  $k_y$  integrals, letting  $\epsilon \rightarrow 0$ , and evaluating the  $\omega'$  integral, we obtain

$$P_{3-D}(x_a, y, z, t) \sim \frac{-i\rho_0 w_0 U \sqrt{2M}}{\pi \sqrt{x_a^2 + y^2 + z^2}} \exp \left\{ \frac{i\omega}{1 + M \cos \theta_a \sin \psi} \left[ t - \frac{b\sqrt{x_a^2 + y^2 + z^2}}{c_0} \right] \right\} \cdot \frac{D(\theta_a, \psi)}{(1 + M \cos \theta_a \sin \psi)^2} \quad (42)$$

$\sqrt{x_a^2 + y^2 + z^2} \rightarrow \infty$

where the distance  $r_a = \sqrt{x_a^2 + y^2 + z^2}$  and the angles  $\theta_a, \psi$  shown in Fig. 6 define the position of the listener in the acoustic reference frame by means of spherical coordinates.  $\theta_a$  denotes  $\tan^{-1}(z/x_a)$ .  $D(\theta_a, \psi)$  is the three-dimensional acoustic directivity function not including the factor  $(1 + M \cos \theta_a \sin \psi)^{-2}$  which gives the usual forward enhancement of the acoustic signal from a moving source. Incidentally,  $1 + M \cos \theta_a \sin \psi$  also gives the Doppler shift which appears in the exponent in Eq. (42). The directivity  $D(\theta_a, \psi)$  was found to be

$$D(\theta_a, \psi) = \frac{\sin \left[ \frac{\omega b}{U} \frac{\ell}{b} \left\{ \frac{M \cos \psi}{1 + M \cos \theta_a \sin \psi} - \tan \Lambda^* \right\} \right]}{\frac{\omega b}{U} \left( \frac{M \cos \psi}{1 + M \cos \theta_a \sin \psi} - \tan \Lambda^* \right)} \frac{I}{\sqrt{1 + M \left\{ 1 - \frac{(1-M^2) \cos^2 \psi}{(1 + M \cos \theta_a \sin \psi)^2} \right\}^{1/2}}} \\ \left\{ \frac{-i \sin \theta_a \sin \psi / \sqrt{2}}{\sqrt{\frac{1}{(1-M^2)} \left\{ 1 - \frac{(1-M^2) \cos^2 \psi}{(1 + M \cos \theta_a \sin \psi)^2} \right\}^{1/2} - \frac{M}{1-M^2} \frac{\cos \theta_a \sin \psi}{1 + M \cos \theta_a \sin \psi}}} + i(1 + M \cos \theta_a \sin \psi) \left\{ 1 - \frac{(1-M^2) \cos^2 \psi}{(1 + M \cos \theta_a \sin \psi)^2} \right\}^{1/4}} \right. \\ \left. \cdot \left( 1 + \sqrt{2} e^{-3\pi i/4} E^* \left[ \frac{2\omega b M}{U} \left( \frac{1}{1-M^2} \left\{ 1 - \frac{(1-M^2) \cos^2 \psi}{(1 + M \cos \theta_a \sin \psi)^2} \right\}^{1/2} - \frac{M^2}{1-M^2} \frac{\cos \theta_a \sin \psi}{1 + M \cos \theta_a \sin \psi} \right) \right] \right) \right\} \quad (43)$$

where the substitution for  $k_y^* = (\omega b/U) \tan \Lambda^*$  has been made.



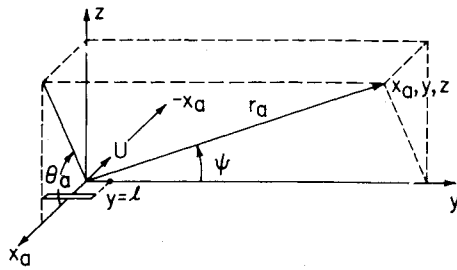


Fig. 6 Spherical coordinate system defining the position of listener in acoustical reference frame.

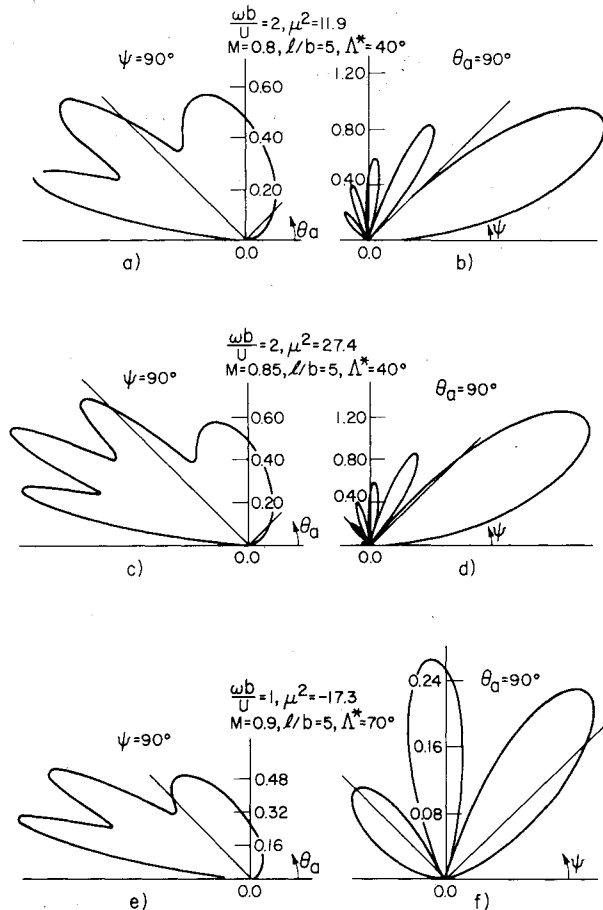


Fig. 7 Magnitude of total acoustic directivity  $|D(\theta_a, \psi)| (1 + M \cos \theta_a \sin \psi)^{-2}$  in acoustic reference frame for the  $\psi = 90$  deg (a,c,e) and  $\theta_a = 90$  deg (b,d,f) planes.

Figures 7a and b are plots of

$$\frac{|D(\theta_a, \psi)|}{(1 + M \cos \theta_a \sin \psi)^2}$$

in the two perpendicular planes given by  $\psi = \pi/2$ ,  $\theta_a$  variable, and  $\theta_a = \pi/2$ ,  $\psi$  variable, respectively. The  $\theta_a = 0$  line in Fig. 7a is in the wake. Figures 7c and d and 7e and f are similar plots for different Mach number and reduced frequency combinations.

## Discussion of Results

### Aerodynamics

Equation (31) gives an approximation to the pressure distribution on an infinite-span wing passing through an oblique gust of short wavelength. This result agrees with that

given in Ref. 9 for the case of zero sweep and collapses to that presented in Ref. 12 for the case of a gust parallel to the wing. We see now precisely how the shortness of the gust's wavelength allows us to consider the edge effects separately: for large  $|\mu|$ , the components of Eq. (31) given in Eqs. (15) and (30) becomes concentrated at the leading edge and at the trailing edge, respectively. The edge separation technique is therefore justified for large values of  $|\mu|$ .

In Ref. 12, Amiet estimates that the cut-off limit for real  $\mu$  is about  $\pi/4$  for the edge separation technique to give good aerodynamic results. In Ref. 9, Adamczyk gives the somewhat lower value of 0.7. Their conclusions are based on comparisons with numerical results due to Graham,<sup>15</sup> for the exact problem. For negative  $\mu^2$  the criterion for smallest allowed value of  $|\mu|$  for which the present two-term theory is good may be somewhat relaxed. Apparently, this is due to the much faster convergence of the trailing-edge solution in this case. Since it was not clear from the literature, however, what the lower bound for  $|\mu|$  should be for  $\mu^2$  negative, we considered only practical cases for which  $|\mu^2| > (\pi/4)^2$ .

### Acoustics

Since the aerodynamic results presented here had already been established elsewhere, the contribution of this paper is really just the acoustic results for the wing-gust interaction. These are given in closed form in Eq. (34) and Eqs. (42) and (43) for the infinite-span (two-dimensional) and the finite-span (three-dimensional) cases, respectively. The results were obtained by approximating the expressions for the pressure in the far-field for the two- and three-dimensional problems by steepest descents and stationary phase, respectively.

Figures 5a and b for the cases of supersonically traveling disturbances ( $M/\sin \Lambda > 1$ ) show that the number of lobes in the two-dimensional directivity  $D(\theta)$  is very sensitive to small Mach number variations. These results predict the directivity of sound in a wind tunnel experiment.

Equation (43) is an approximation to the three-dimensional acoustic directivity  $D(\theta_a, \psi)$  for the passage of a rectangular flat-plate wing of span  $2l$  through a stationary oblique gust. This result is given in the acoustic reference frame. The interaction angle  $\Lambda^*$  and the gust's wavelength are such that  $|\mu^2| = |\mu^2(\Lambda^*)| > (\pi/4)^2$  is satisfied. This way, the  $k_y$ -Fourier components in Eq. (35) individually satisfy the condition of  $|\mu^2| > (\pi/4)^2$ , for the most part.

In Figure 7, the a, c, e plots show the familiar forward enhancement of the acoustic signal from a moving source. The number of lobes is again seen to be a very sensitive function of the Mach number. Figures 7b and d show that when  $\mu(\Lambda^*) > \pi/4$  the radiation becomes highly directional. A real value of  $\mu(\Lambda^*)$  corresponds to a supersonic spanwise-propagation speed of the disturbance due to the wing-gust interaction through the still fluid. In this case, a listener at a general point in the far-field hears sound coming from every point on the planform except the trailing edge. For  $\mu^2(\Lambda^*) < -(\pi/4)^2$ , Fig. 7f shows that radiation has no single preferred direction in the  $\theta_a = \pi/2$  plane. This case corresponds physically to a subsonic spanwise propagation speed of the disturbance due to the passage of a finite-span wing through a stationary gust. In this case, a listener hears sound coming from only the tip edges of the wing.

### Acknowledgment

This work was supported by NASA Grant NSG-2142.

### References

- Amiet, R. K., "Acoustic Radiation from an Airfoil in a Turbulent Stream," *Journal of Sound and Vibration*, Vol. 41, No. 4, Aug. 1975, pp. 407-420.
- Landahl, M. T., *Unsteady Transonic Flow*, Pergamon Press, N.Y., 1961, pp. 28-29.

<sup>3</sup>Landahl, M. T., "Theoretical Studies of Unsteady Transonic Flow—IV. The Oscillating Rectangular Wing with Control Surface," Aeronautical Research Institute of Sweden (FFA), Rept. 80, 1958.

<sup>4</sup>Goldstein, M. E., *Aeroacoustics*, McGraw-Hill, N.Y., 1976, pp. 130-139.

<sup>5</sup>Widnall, S. E., "Helicopter Noise Due to Blade-Vortex Interaction," *The Journal of the Acoustical Society of America*, Vol. 50, No. 1, 1971, Pt. 2.

<sup>6</sup>Wolf, T. and Widnall, S. E., "The Effect of Tip Vortex Structure on Helicopter Noise due to Blade-Vortex Interaction," MIT Fluid Dynamics Research Laboratory, Rept. 78-2, 1978.

<sup>7</sup>Kaji, S., "Non-Compact Source Effect on the Prediction of Tone Noise from a Fan Rotor," AIAA Paper 75-446, 2nd Aeroacoustics Conference, March 24-26, 1975.

<sup>8</sup>Adamczyk, J. J. and Brand, R. S., "Scattering of Sound by an Aerofoil of Finite Span in a Compressible Stream," *Journal of Sound and Vibration*, Vol. 25, No. 1, Nov. 1972, pp. 139-156.

<sup>9</sup>Adamczyk, J. J., "The Passage of an Infinite Swept Airfoil through an Oblique Gust," NASA CR-2395, May 1974.

<sup>10</sup>Paterson, R. W. and Amiet, R. K., "Acoustic Radiation and Surface Pressure Characteristics of an Airfoil due to Incident Tur-

bulence," AIAA Paper 76-571, 3rd Aeroacoustics Conference, July 20-23, 1976.

<sup>11</sup>Amiet, R. K., "Noise Produced by Turbulent Flow into a Propeller or Helicopter Rotor," *AIAA Journal*, Vol. 15, March 1977, pp. 307-308.

<sup>12</sup>Amiet, R. K., "High Frequency Thin Airfoil Theory for Subsonic Flow," *AIAA Journal*, Vol. 14, Aug. 1976, pp. 1076-1082.

<sup>13</sup>Noble, B., *Methods based on the Wiener-Hopf Technique*, International series of Monographs on Pure and Applied Mathematics, Pergamon Press, N.Y., 1958, pp. 34-35.

<sup>14</sup>Whitham, G. B., *Linear and Non-Linear Waves*, Wiley, N.Y., 1974, p. 382.

<sup>15</sup>Graham, J.M.R., "Similarity Rules for Thin Aerofoils in Non-Stationary Flows," *Journal of Fluid Mechanics*, Vol. 43, Oct. 1970, pp. 753-766.

<sup>16</sup>Carrier, Krook, and Pearson, *Functions of a Complex Variable, Theory and Technique*, McGraw-Hill, N.Y., 1966, pp. 382-383.

<sup>17</sup>Sommerfeld, A., *Partial Differential Equations in Physics*, Academic Press, N.Y., 1964, p. 89.

## *From the AIAA Progress in Astronautics and Aeronautics Series . . .*

### **INTERIOR BALLISTICS OF GUNS—v. 66**

*Edited by Herman Krier, University of Illinois at Urbana-Champaign,  
and Martin Summerfield, New York University*

In planning this new volume of the Series, the volume editors were motivated by the realization that, although the science of interior ballistics has advanced markedly in the past three decades and especially in the decade since 1970, there exists no systematic textbook or monograph today that covers the new and important developments. This volume, composed entirely of chapters written specially to fill this gap by authors invited for their particular expert knowledge, was therefore planned in part as a textbook, with systematic coverage of the field as seen by the editors.

Three new factors have entered ballistic theory during the past decade, each so happened from a stream of science not directly related to interior ballistics. First and foremost was the detailed treatment of the combustion phase of the ballistic cycle, including the details of localized ignition and flame spreading, a method of analysis drawn largely from rocket propulsion theory. The second was the formulation of the dynamical fluid-flow equations in two-phase flow form with appropriate relations for the interactions of the two phases. The third is what made it possible to incorporate the first two factors, namely, the use of advanced computers to solve the partial differential equations describing the nonsteady two-phase burning fluid-flow system.

The book is not restricted to theoretical developments alone. Attention is given to many of today's practical questions, particularly as those questions are illuminated by the newly developed theoretical methods. It will be seen in several of the articles that many pathologies of interior ballistics, hitherto called practical problems and relegated to empirical description and treatment, are yielding to theoretical analysis by means of the newer methods of interior ballistics. In this way, the book constitutes a combined treatment of theory and practice. It is the belief of the editors that applied scientists in many fields will find material of interest in this volume.

385 pp., 6 × 9, illus., \$25.00 Mem., \$40.00 List

TO ORDER WRITE: Publications Dept., AIAA, 1290 Avenue of the Americas, New York, N. Y. 10019